International Journal of Biomass Utilization and Sustainable Energy
Volume 2, 2024 [30-41]

Activated Carbon derived from Jackfruit Seeds for Oil Adsorption

Zi Ching Chan[1], Hairul Nazirah Abdul Halim[1,2*], Siti Khalijah Mahmad Rozi[1,2]

[1]Faculty of Chemical Engineering & Technology, Universiti Malaysia Perlis (UniMAP), 02600 Arau, Perlis, Malaysia

[2]Centre of Excellence for Biomass Utilization (CoEBU), Universiti Malaysia Perlis, 02600 Arau, Perlis, Malaysia

ABSTRACT

Activated carbons (AC) are widely used as adsorbents for treating oily wastewater. An effective, cheap and environmental-friendly method for oil adsorption by using AC derived from jackfruit seeds (JS) was developed in this study. The JS were chemically activated with different concentrations (10 wt.% and 15 wt.%) of chemical activating agents (H_3PO_4 and $ZnCl_2$) to produce activated carbon. The optimum conditions for developing AC from JS with the highest oil adsorption capacity was found using 15 wt.% $ZnCl_2$, and carbonised at 500°C resulting in maximum adsorption capacity of 0.8621 g/g. Raw JS and jackfruit seed-derived activated carbon (JSAC) were characterized by Fourier Transform Infrared Spectroscopy and Scanning Electron Microscopy analysis. The influence of process parameters such as contact times (0 – 240 minutes), adsorbent dosages (0.5 – 2.5 g) and adsorption temperatures (25 – 65 °C) for oil adsorption were investigated. The results showed that the optimum parameters for maximum adsorption capacity were as follows; 120 minutes of contact time, adsorbent dosage of 1.5 g and at 35 °C. At this condition, the highest oil adsorption capacity was achieved at 1.5674 g/g. The adsorption kinetic studies depicted that the oil adsorption mechanism was represented by pseudo-second-order kinetic model which implies that the adsorption is a chemisorption process. Jackfruit seeds had been proven to have the capability as an effective adsorbent for oil adsorption.

Keywords: Activated carbon, Jackfruit seeds, Adsorption, Oil Pollutant, Kinetics

1. INTRODUCTION

Oil pollution is a serious environmental disaster caused by the operational and accidental discharge of poorly treated wastewater into the coastal environment. Oil pollution is defined as release of hydrocarbons into an aquatic environment caused by human activities that can contribute to a number of issues on the environment and economy (Li et. al, 2016). In addition, the main source of such pollution was generated by liquid hydrocarbons discharged into the receiving coastal environment (Worthington et. al, 2018). Oil pollution has long become a major concern worldwide. Malaysia has started the journey of preventing and controlling oil pollution since 1975 when a National Oil Spill Contingency Plan (NOSCP) has been established to minimize oil leaks in the Straits of Malacca. For the past 50 years, oil spillage in the coastal and marine environment has continued, gaining concern with growth in industrial production and urbanization. Urban and industrial runoff contributes a very high percentage which is 77 % to marine pollution (Zafirakou et. al, 2018).

*Corresponding author: hairulnazirah@unimap.edu.my

Untreated wastewater discharge sometimes contains oil and grease which are toxic substances to the coastal environment. The oily waste spread out across the water surface, posing a threat to marine life by preventing oxygen from reaching them. In conjunction with NOSCP, Malaysia aims to lessen the environmental damage caused by oil spills in the sea by utilizing agricultural wastes.

The most common and efficient technique that has been acknowledged for oily wastewater treatment is adsorption. Adsorption using activated carbon only requires a low concentration of carbonaceous material for removal purposes, thus low space requirement (Ani et. al, 2020). Conventional activated carbon available in the market is expensive, thus not economical for oil adsorption. Activated carbon prepared from natural carbon-rich materials including agricultural and household wastes has received attention as they have high potential to effectively eliminate contaminants from wastewater. Biomass-derived adsorbents with low costs symbolize a successful clean technology. Converting such unwanted biomass into profitable products could be a viable option for reducing pollution and improving waste management as it enhances the reduction of waste without the incineration process, thus reducing greenhouse gas emissions.

Based on previous studies, jackfruit seed (JS) was proven to have high adsorption capacity for the removal of pollutants from wastewater (Azreen et. al, 2017; Kooh et. al, 2016; Behera, 2014). JS is a carbon-rich organic material and is suitable to be converted into activated carbon. In jackfruit plantation, some of the JS are used for planting purposes, but most of them are disposed off and utilized for incineration to generate electricity. This study determines the ability of JS to act as a low-cost adsorbent for the treatment of oily wastewater, hence encouraging agricultural waste utilisation in Malaysia.

2. MATERIALS AND METHODS

2.1 Sample Preparation

JS were obtained from local markets in Kangar, Perlis and used as the raw material for the synthesis of activated carbon. The seeds were washed with distilled water to remove impurities, oven-dried at 100 °C for 24 hours, and ground into powder. Then, the samples were sieved (1,000 μm) and stored in zipper bags for further use.

2.2 Chemical activation and carbonization

The chemical activation method was employed using 10 wt. % and 15 wt. % of phosphoric acid (H_3PO_4) (Bendosen, Malaysia), and zinc chloride ($ZnCl_2$)(HmbG, Malaysia). The samples were soaked in these chemical activating agents with an impregnation ratio of 1:1 on weight basis for 24 hours at room temperature. Then, the samples were filtered. The slurries obtained were heated in the oven at 100°C for 1 hour, and were carbonized in the furnace at 300 °C, 400 °C and 500 °C for 1.5 hours (Jutakridsada et. al, 2015). Once the activation process was completed, the activated carbon formed was collected and cooled at room temperature. After carbonization, the samples were washed with distilled water repeatedly until pH 6 – 7 was obtained (Anwana Abel et. al, 2020).

2.3 Characterization of jackfruit seeds

The samples were dried and mixed with potassium bromide prior to functional groups analysis using the Fourier Transform Infrared (FTIR) (PerkinElmer Spectrum 65 FTIR Spectrometer, USA) at wavelength between 650 cm^{-1} to 4000 cm^{-1}. Surface morphology analysis was carried out on the jackfruit seeds before and after chemical activation using a Scanning Electron Microscope (SEM) (Hitachi TM3000, Japan) under vacuum and accelerating voltage of 5 kV.

2.4 Batch adsorption test

First, adsorption tests were done to compare the performance of raw JS and jackfruit seed-derived activated carbon (JSAC) using H_3PO_4 and $ZnCl_2$ at 300 °C, 400 °C and 500 °C. Before running the test, 1 g of each adsorbent was sealed into several tea bags with the dimension of 5 cm × 7 cm. The teabag was soaked in 20 g of cooking oil in a 100 mL beaker for 150 mins at room temperature (25 ˚C). Then, the teabags were removed from the beakers to allow the oil from the teabag to drip into a filter funnel for 15 mins. The mass of the adsorbent before and after adsorption test were measured and recorded. All tests were done in triplicate and the mean values were calculated. The best adsorbent with the highest oil adsorption capacity was further studied to observe the effects of the following process parameters.

2.4.1 Effect of contact times

The effect of contact time between JSAC adsorbent and oil substances were carried out from 0 to 240 minutes with 30 mins increment, at room temperature (Anwana et. al, 2020). Eight sets of beakers were prepared for the purpose of sampling every 30 minutes. First, 1 g of AC was weighed and packed in a nylon teabag (5 x 7 cm). The teabag was soaked in 20 g of oil in a 100 mL glass beaker. The experiments were conducted without agitation at room temperature. At every interval of 30 minutes, the teabag was removed from the glass beaker, and the oil was left to drip from the teabag into the filter funnel for 15 mins. The teabag was subsequently weighed. The steps of taking out the tea bag, dripping the oil and weighing were repeated after every specific time of 30 minutes until 240 minutes. Each experiment was conducted in triplicates and the value of mean and standard deviation of the adsorption capacity were calculated.

2.4.2 Effect of adsorbent dosages

The effect of adsorbent dosage on oil removal was performed using 0.5, 1.0, 1.5, 2.0, and 2.5 g of JSAC (Anwana et. al, 2020). The teabags with the dimensions of 5 cm × 7 cm were filled with different adsorbent dosages and left in contact with 20 g of oil for 1 hour without agitation at room temperature. After an hour, each teabag was taken out of the oil and the oil was left to drip from the teabag into the filter funnel. The teabag was weighed after each experiment. The experiments were conducted in triplicates, and the value of mean and standard deviation of the adsorption capacity were calculated.

2.4.3 Effect of adsorption temperatures

Different temperature for the water bath were set at 25, 35, 45, 55, and 65 °C, where a beaker was filled with 20 g of oil and a teabag containing 1 g of adsorbent was placed inside (Anwana et. al, 2020). The adsorption of oil into the sample was allowed to occur for 2 hours without agitation. At the end of the experiment, the teabag was taken out from the beaker and the oil was left to drip from the teabag into the filter funnel, prior to weighing the teabag. Each experiment was conducted in triplicates, and the value of mean and standard deviation of the adsorption capacity were calculated.

2.5 Data analysis

2.5.1 Adsorption capacity

Adsorption capacity is the amount of adsorbate taken up by the adsorbent per unit mass of the adsorbent. The adsorption capacity, q, was obtained using Equation 1:

$$q = \frac{M_f(g) - M_i(g)}{M_i(g)} \quad (1)$$

where, M_i (g) and M_f (g) are the mass of the adsorbent before and after adsorption, respectively.

2.5.2 Adsorption kinetic study

To investigate the mechanism of adsorption, the following kinetic rate equations were used to test the experimental data. The kinetics data were evaluated using pseudo-first-order (Equation 2) and pseudo-second-order (Equation 4).

Pseudo-first-order kinetic model:

$$\frac{dq_t}{d_t} = k_1(q_e - q_t) \tag{2}$$

where, q_e (mg/t) and q_t (mg/t) are the amount of adsorbed oil at equilibrium and at time t respectively while k_1 is the rate constant of pseudo-first-order adsorption. The equation is then integrated to the following equation for boundary conditions (t = 0, q_t = 0 and t = t, $q_e = q_t$):

$$\ln(q_e - q_t) = \ln q_e - k_1 t \tag{3}$$

The adsorption rate at constant value, k_1 and adsorption amount of q_e, can be calculated by plotting $\ln(q_e - q_t)$ against time, t.

Pseudo-second-order kinetic model:

$$\frac{dq_t}{d_t} = k_2(q_e - q_t)^2 \tag{4}$$

where, q_e (mg/t) and q_t (mg/t) are the amount of adsorbed oil at equilibrium and at time t, respectively, while k_2 is the rate constant of pseudo-second-order adsorption. After integration for boundary condition (t = 0, q_t = 0 and t = t, $q_e = q_t$), the equation is rearranged to obtain linear form as follows:

$$\frac{t}{q_t} = \frac{1}{k_2 q_e^2} + \frac{t}{q_e} \tag{5}$$

A graph of $\frac{t}{q_t}$ against t will be plotted to determine the values of k_2 and q_e, through the intercept and slope of the graph.

The graphs obtained by pseudo-first-order equation as well as pseudo-second-order equation were compared to determine which model is best-fit for the adsorption of oil onto jackfruit seed-derived activated carbon. The one with high correlation coefficient (R^2) is the most suitable model.

3. RESULTS AND DISCUSSION

3.1 Batch experiment for preliminary performance of oil adsorption

Batch experiments were conducted to determine the oil adsorption capacities of raw JS and JSAC using different concentrations of chemical activating agents which were $ZnCl_2$ and H_3PO_4 at 300°C, 400°C and 500°C. The selected adsorbent were further tested on the effects of experimental parameters such as contact time, adsorbent dosage and adsorption temperature. Figure 1 shows the adsorption capacities of Raw JS and JS activated carbon (JSAC) produced at different conditions.

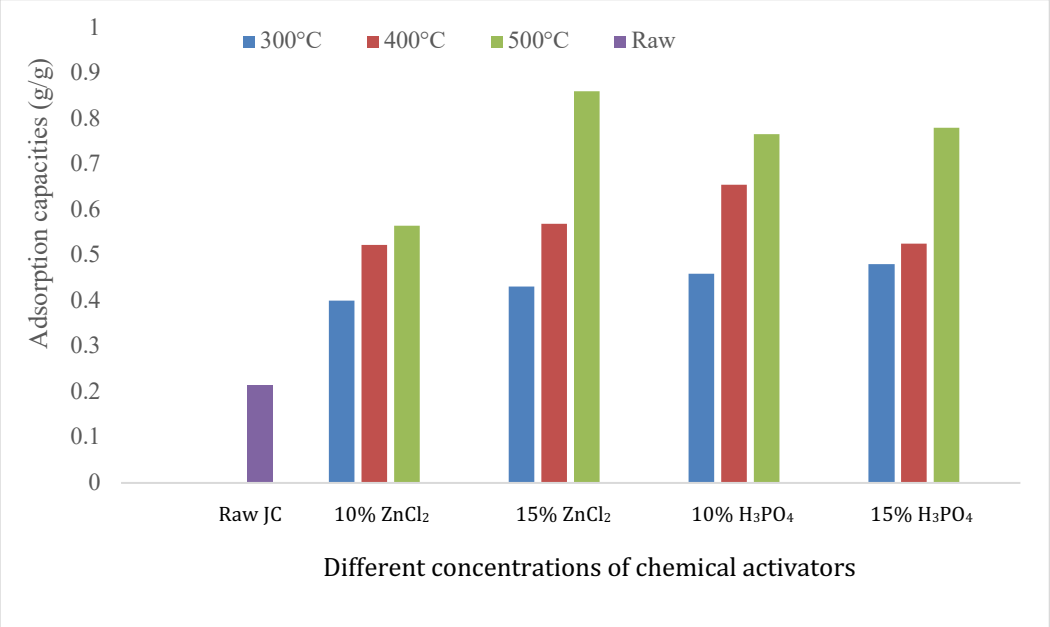

Figure 1: Adsorption capacities of raw jackfruit seeds and different JSAC.

The oil adsorption capacity of raw JS was 0.2141 g/g. Based on Figure 1, the highest adsorption capacity was 0.8621 g/g obtained by JSAC activated by 15 wt % $ZnCl_2$ at carbonisation temperature of 500°C. Meanwhile, the JSAC with the lowest adsorption capacity was activated with 10 wt. % $ZnCl_2$ at carbonisation temperature of 300°C. JSAC impregnated with $ZnCl_2$ as activating agent showed higher oil adsorption capacity compared to the ones activated with H_3PO_4. This might be due to $ZnCl_2$ acting as a booster that accelerates the breakdown of carbonaceous materials during carbonization, promotes pore formation, and improves carbon output (Al-Lagtah et. al, 2019). These findings were in line with Ukanwa et. al, (2019) which also found $ZnCl_2$ as the best chemical activator among the tested activation agents such as H_3PO_4 and KOH.

The role of activation agents and carbonization temperature were clearly seen by comparing the adsorption capacity of JSAC and raw JS. The lowest adsorption capacity of the raw JS was due to the absence of large pores, which is important for oil adsorption. Meanwhile for JSAC, higher adsorption capacity was contributed by the large pores developed during chemical activation and carbonization processes (Liu et. al, 2021). The results also showed the importance of carbonization temperature on the production of activated carbon. According to earlier research, chemically activated agricultural wastes carbonized at 500°C always achieve the highest dye adsorption efficiency (Ukanwa et. al, 2019).

3.2 Characterization of Prepared Adsorbents

3.2.1 Functional groups analysis

The functional groups of raw JS were examined and compared before and after chemical activation. The spectra of raw JS and JSAC are illustrated in Figure 2. The FTIR spectrum of raw JS shows broad absorption band around 3307.8 cm^{-1}, indicating the presence of hydroxyl and amine groups. Moreover, the band at 2925.2 cm^{-1} for raw JS is attributed to C – H stretching of the methyl group (Ateş & ÖZcan, 2018). The peaks at 1635.03 cm^{-1} and 1412.41 cm^{-1} suggest the presence of N – H bending and phenyl group of the biomass of raw JS (Chaudhary et. al, 2020; Kooh et. al, 2016). Moreover, C – O stretching is observed at the peak of 1078.38 cm^{-1} and strong peak at 1020.57 cm^{-1} is for aliphatic ether.

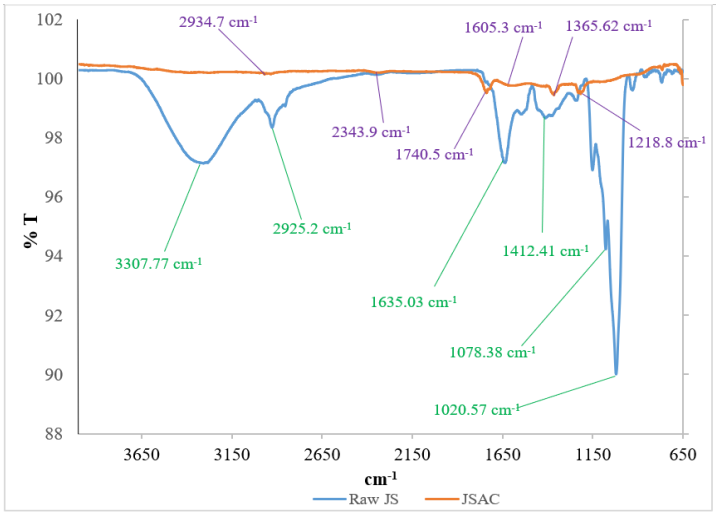

Figure 2: FTIR spectrum of raw jackfruit seeds (JS) and jackfruit seed-derived activated carbon (JSAC)

After chemical activation with $ZnCl_2$, some of the absorption bands decreased or disappeared on the spectra of activated carbon. JSAC shows low intensity of the O – H absorption band suggesting the dehydration of cellulose and lignin components by the chemical activating agent (Bakti & Gareso, 2018). The ester linkage of the carboxyl group and C=C stretching vibration are seen at 1740.5 cm^{-1} and 1605.3 cm^{-1}, respectively. The peak at 1218.8 cm^{-1} may be due to deformation of C – O. When heat was applied to the sample during the activation process, some of the hydrophilic functional groups from the raw material were discharged as volatile components resulting the loss of some functional groups, including hydroxyl, suggesting the obtained JSAC has enhanced hydrophobic properties which is suitable for oil adsorption process.

3.2.2 Surface morphology analysis before and after chemical activation

Figure 3 shows the SEM images of raw JS at magnifications of 300 and 500 times. The surface of raw JS showed no visible pores on its slightly rough surface before chemical activation.

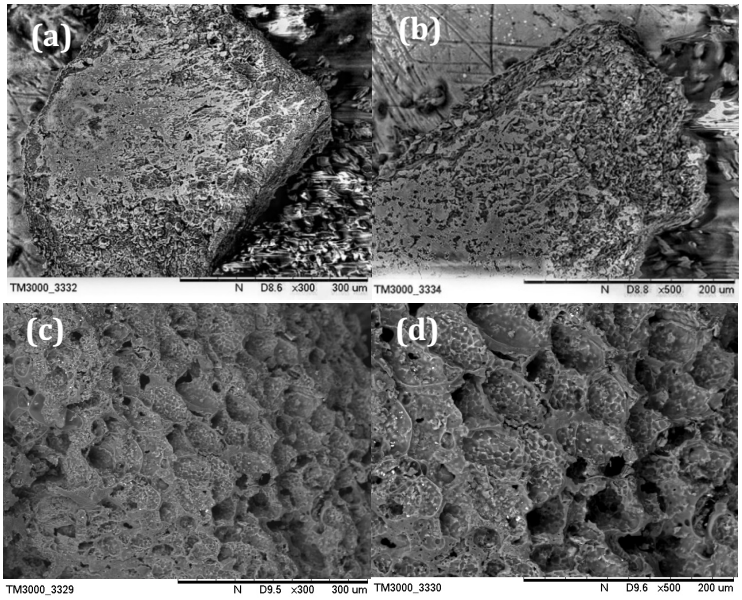

Figure 3: SEM images of raw JS at magnifications of **(a)** × 300 and **(b)** × 500 and JSAC at magnifications of **(c)** × 300 and **(d)** × 500.

After chemical activation, JSAC demonstrated a very rough surface with numerous large pores with honeycomb-like surface. This result suggests that the carbonization and chemical activation processes caused the formation of pores on raw JS. Thermal stresses caused by the high temperature led to formation of cracks and crevices which eventually lead to formation of pores (Ateş & ÖZcan, 2018). Similar results were found when using palm kernel shells (Ramli & Ghazi, 2020). The pores on the surface of JSAC were useful for enhanced oil molecules during adsorption process.

3.3 Parametric studies

3.3.1 Effect of contact time

The effect of contact time on oil adsorption for 1 g of synthesized adsorbent is depicted in Figure 4.

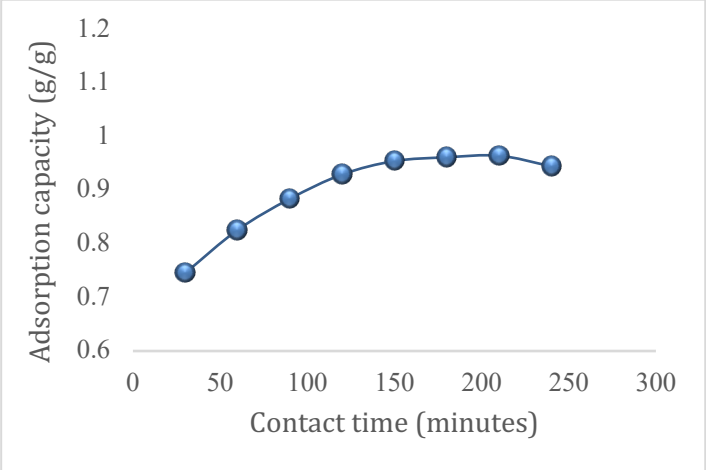

Figure 4: The effect of contact time on oil adsorption capacity

The effect of contact time was studied from 30 minutes to 240 minutes. From Figure 4, it can be observed that rapid oil adsorption occurred during the first 120 minutes. This was due to the availability of a large amount of numerous active sites (Sharma et. al, 2019). The rate of adsorption becomes slower near the equilibrium after 120 minutes due to lesser availability of active sites and no further adsorption occurred. The equilibrium time for oil adsorption was 150 – 210 minutes. At 120 minutes, the highest adsorption capacity was achieved at 0.9645 g/g. However, when contact time increased, the oil accumulated in the active sites on the adsorbent and then equilibrium was reached. After equilibrium, there was a slightly drop in adsorption capacity at 240 minutes which might be due to the filled active sites with oil molecules resulting in no additional adsorption (Behera, 2014).

3.3.2 Effect of adsorbent dosages

The relationship between oil adsorption capacity and adsorbent dosage was investigated in the range of 0.5 to 2.5 g. Figure 5 depicted that the oil adsorption capacity increased with an increase in dosage of adsorbent due to the increasingly available active sites for oil adsorption on the surface of JSAC. The maximum adsorption capacity of JSAC was found at 1.5 g which is 1.5674 g/g, attributed to the saturation of all binding sites for oil components on the surface of JSAC during adsorption. Oil removal efficiency was slightly declined after 1.5 g due to the excess adsorbent dosage, which may lead to aggregation of the adsorbent particles, thus expanding their particle size (Mishra et. al, 2019). Hence, their surface area was reduced, leading to the reduction in the availability of binding sites for oil components toward the surface of adsorbent and drop in adsorption efficiency (Singh et. al, 2019). Therefore, 1.5 g of JSAC is the optimum dosage for oil adsorption.

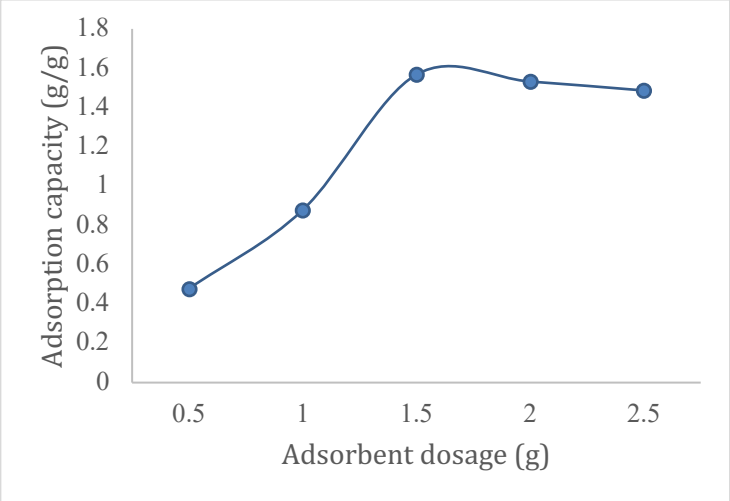

Figure 5: The effect of adsorbent dosage on oil adsorption capacity.

3.3.3 Effect of adsorption temperature

Temperature is a critical factor that influences adsorption capability. The effect of temperature on adsorption capacity was studied over the temperature of 25 °C to 65 °C. Figure 6 represents the adsorption of oil by JSAC at different temperatures; 25, 35, 45, 55 and 65 °C. The adsorption capacity was the highest when the adsorption was conducted between 25 and 35 °C. At 35 °C, the adsorption capacity achieved was 0.9764 g/g. When the temperature was further increased, there was a reduction in adsorption capacity, showing that temperature is inversely proportional to the extent of adsorption.

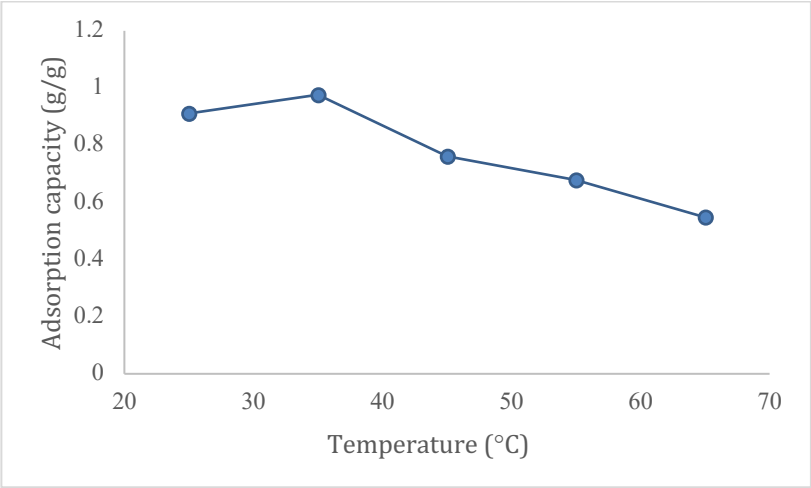

Figure 6: The effect of adsorption temperature on oil adsorption capacity.

3.4 Adsorption kinetics

Pseudo-first and -second order kinetic models were employed to discuss the controlling mechanism. The models were used to find out the most suitable adsorption mechanism utilized by JSAC to adsorb oil. Figure 7 and 8 depicted the graphs obtained by equations of pseudo-first-order and pseudo-second-order kinetic model, respectively.

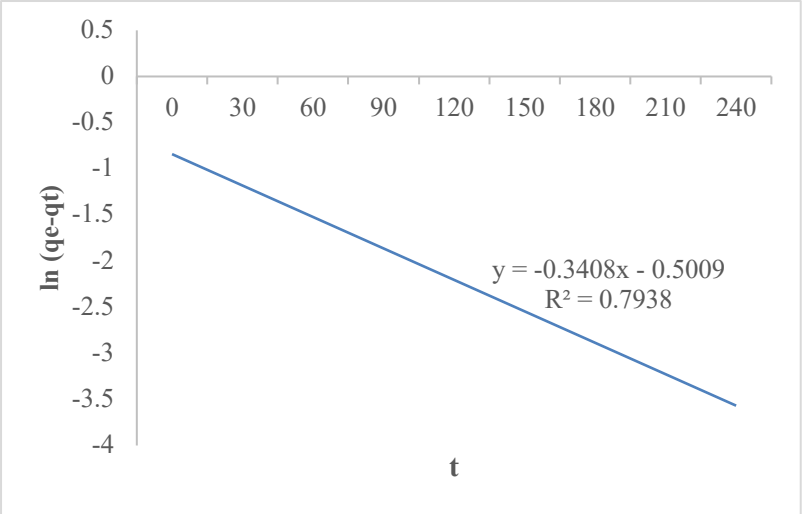

Figure 7: Pseudo-first-order kinetic model.

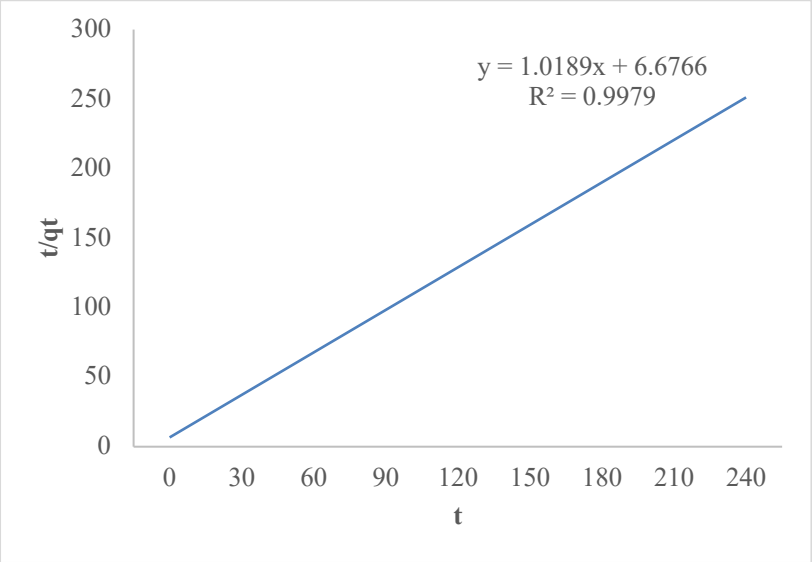

Figure 8: Pseudo-second-order kinetic model.

Pseudo-first-order kinetic model was plotted by using ln (q_e - q_t) against contact time, t whereas pseudo-second-order kinetic model was plotted by using t/q_t as y-axis and contact time, t as x-axis. The coefficient of determination, R^2 for pseudo-second-order kinetic model was 0.9979, compared to R^2 for pseudo-first-order kinetic model which was 0.7938. It indicated that pseudo-second-order kinetic model provides a good correlation on the adsorption of oil by using JSAC. It suggests that chemisorption process could be the rate limiting step which involves covalent forces through sharing or exchange of electrons between the adsorbents and cooking oil molecules due to the modified adsorbents' high hydrophobic nature. Previous research has revealed that the pseudo-second-order model is considered as the most suitable for kinetic results for oil adsorption (Sun et. al, 2017; Aliakbarian et. al, 2015). Table 1 shows the important data for pseudo-first and -second order kinetic models. It can be observed that pseudo-second-order kinetic model has a better set of data compared to that of pseudo-first-order kinetic model.

Table 1: Important data for pseudo-first and -second order kinetic models.

Pseudo-first-order kinetic model		**Pseudo-second-order kinetic model**	
R^2	0.7938	R^2	0.9979
q_e	1.65021	q_e	0.98145
k_1	0.3408	k_2	0.15549

4. CONCLUSION

The study has highlighted the synthesis of a new adsorbent for oil adsorption. The JSAC were successfully produced and studied for oil removal application. The highest oil adsorption capacity was found at chemical activation with 15 wt. % $ZnCl_2$ and carbonization temperature at 500°C. This condition has resulted in a maximum adsorption capacity of 0.8621 g/g. Results from FTIR proved that the synthesized adsorbent consists of C=C, and C–O groups as dominant functional groups which are responsible for oil adsorption. Moreover, the disappearance (very low intensity) of the O-H absorption band assigned that the hydroxyl groups were successfully reduced by the chemical impregnation with $ZnCl_2$. Hydroxyl and aliphatic groups from the JS were decomposed during the activation process enhancing the pore formation. The most suitable conditions for the maximum adsorption capacity of 20 g of cooking oil onto JSAC was 120 minutes of contact time, adsorbent dosage of 1.5 g and at 35°C. At optimum condition, the highest adsorption capacity achieved was 1.5674 g/g. The oil adsorption mechanism can be represented by pseudo-second-order kinetic model. It implies that the adsorption is a chemisorption process, which involves covalent forces through the sharing or exchange of electrons between the adsorbents and cooking oil molecules, and transfer of oil molecules to adsorbent surface is fast due to the modified adsorbents' high hydrophobic nature.

ACKNOWLEDGMENT

This study was supported by the Faculty of Chemical Engineering & Technology, Universiti Malaysia Perlis (UniMAP).

REFERENCES

Aliakbarian, B., Casazza, A. A., & Perego, P. (2015). Kinetic and Isotherm Modelling of the Adsorption of Phenolic Compounds from Olive Mill Wastewater onto Activated Carbon. *Food Technol Biotechnol, 53*, 207–214.

Al-Lagtah, N. M., Al-Muhtaseb, A. H., Ahmad, M. N., & Salameh, Y. (2019). Elaboration and characterisation of novel low-cost adsorbents from grass-derived sulphonated lignin. *Arabian Journal of Chemistry*, *12*(8), 2943–2958.

Ani, J. U., Akpomie, K. G., Okoro, U. C., Aneke, L. E., Onukwuli, O. D., & Ujam, O. T. (2020). Potentials of activated carbon produced from biomass materials for sequestration of dyes, heavy metals, and crude oil components from aqueous environment. *Applied Water Science*, *10*, 2.

Anwana Abel, U., Rhoda Habor, G., & Innocent Oseribho, O. (2020). Adsorption Studies of Oil Spill Clean-up Using Coconut Coir Activated Carbon (CCAC). *American Journal of Chemical Engineering*, *8*, 36.

Ateş, F., & ÖZcan, Z. (2018). Preparation and Characterization of Activated Carbon from Poplar Sawdust by Chemical Activation: Comparison of Different Activating Agents and Carbonization Temperature. *European Journal of Engineering Research and Science*, *3*, 6–11.

Azreen, I., Lija, Y., & Zahrim, A. Y. (2017). Ammonia nitrogen removal from aqueous solution by local agricultural wastes. *IOP Conference Series: Materials Science and Engineering*, *206*, 12.

Bakti, A. I., & Gareso, P. L. (2018). Characterization of Active Carbon Prepared from Coconuts Shells using FTIR, XRD and SEM Techniques. *Jurnal Ilmiah Pendidikan Fisika Al-Biruni*, *7*(1), 33–39.

Behera, R. (2014). *Adsorption studies of malachite green using activated carbon prepared from jackfruit seeds.* [bachelor of technology thesis*,* National Institute of Technology Rourkela, India].

Chaudhary, R., Maji, S., Shrestha, R. G., Shrestha, R. L., Shrestha, T., Ariga, K., & Shrestha, L. K. (2020). Jackfruit Seed-Derived Nanoporous Carbons as the Electrode Material for Supercapacitors. *C*, *6*(4), 73.

Jutakridsada, P., Prajaksud, C., Kuboonya-Aruk, L., Theerakulpisut, S., & Kamwilaisak, K. (2015). Adsorption characteristics of activated carbon prepared from spent ground coffee. *Clean Technologies and Environmental Policy*, *18*, 639–645.

Kooh, M. R. R., Dahri, M. K., & Lim, L. B. L. (2016). Jackfruit seed as a sustainable adsorbent for the removal of rhodamine B dye*. Journal of Environment & Biotechnology*.

Li, P., Cai, Q., Lin, W., Chen, B., & Zhang, B. (2016). Offshore oil spill response practices and emerging challenges. *Marine Pollution Bulletin*, *110*, 6–27.

Liu, W., Zhang, Y., Wang, S., Bai, L., Deng, Y., & Tao, J. (2021). Effect of Pore Size Distribution and Amination on Adsorption Capacities of Polymeric Adsorbents. *Molecules*, *26*(17), 5267.

Mishra, S., Yadav, S. S., Rawat, S., Singh, J., & Koduru, J. R. (2019). Corn husk derived magnetized activated carbon for the removal of phenol and para-nitrophenol from aqueous solution: Interaction mechanism, insights on adsorbent characteristics, and isothermal, kinetic and thermodynamic properties. *Journal of Environmental Management*, *246*, 362–373.

Ramli, A. N., & Ghazi, R. M. (2020). Removal of Oil and Grease in Wastewater using Palm Kernel Shell Activated Carbon. *IOP Conference Series: Earth and Environmental Science*, *549*, 012064.

Sharma, M., Joshi, M., Nigam, S., Avasthi, D. K., Adelung, R., Srivastava, S. K., & Mishra, Y. K. (2019). Efficient oil removal from wastewater based on polymer coated superhydrophobic tetrapodal magnetic nanocomposite adsorbent. Applied Materials Today, 17, 130–141.

Singh, H., Jain, A., Kaur, J., Arya, S. K., & Khatri, M. (2019). Adsorptive removal of oil from water using SPIONs–chitosan nanocomposite: kinetics and process optimization. Applied Nanoscience, 10(4), 1281–1295.

Sun, G. Z., Chen, X. G., Zhang, J., Feng, C., & Cheng, X. J. (2017). Adsorption characteristics of residual oil on amphiphilic chitosan derivative. *Water Science Technology, 61*, 2363-74.

Ukanwa, K., Patchigolla, K., Sakrabani, R., Anthony, E., & Mandavgane, S. (2019). A Review of Chemicals to Produce Activated Carbon from Agricultural Waste Biomass. *Sustainability*, *11*(22), 6204.

Worthington, M. J. H., Shearer, C. J., Esdaile, L. J., Campbell, J. A., Gibson, C. T., Legg, S. K., Yin, Y., Lundquist, N. A., Gascooke, J. R., Albuquerque, I. S., Shapter, J. G., Andersson, G. G., Lewis, D. A., Bernardes, G. J. L., & Chalker, J. M. (2018). Sustainable Polysulfides for Oil Spill Remediation: Repurposing Industrial Waste for Environmental Benefit. *Advanced Sustainable Systems*, *2*, 1800024.

Zafirakou, A., Themeli, S., Tsami, E., & Aretoulis, G. (2018). Multi-Criteria Analysis of Different Approaches to Protect the Marine and Coastal Environment from Oil Spills. *Journal of Marine Science and Engineering*, *6*, 125.